INL/CON-09-17224
PREPRINT

# Benchmark Evaluation of the Start-Up Core Reactor Physics Measurements of the High Temperature Engineering Test Reactor

## PHYSOR 2010

John D. Bess

May 2010

*PHYSOR 2010 – Advances in Reactor Physics to Power the Nuclear Renaissance*
Pittsburgh, Pennsylvania, USA, May 9-14, 2010, on CD-ROM, American Nuclear Society, LaGrange Park, IL (2010)

# BENCHMARK EVALUATION OF THE START-UP CORE REACTOR PHYSICS MEASUREMENTS OF THE HIGH TEMPERATURE ENGINEERING TEST REACTOR

**John Darrell Bess**
Idaho National Laboratory
PO Box 1625, Idaho Falls, ID 83415-3855
John.Bess@inl.gov

## ABSTRACT

The benchmark evaluation of the start-up core reactor physics measurements performed with Japan's High Temperature Engineering Test Reactor, in support of the Next Generation Nuclear Plant Project and Very High Temperature Reactor Program activities at the Idaho National Laboratory, has been completed. The evaluation was performed using MCNP5 with ENDF/B-VII.0 nuclear data libraries and according to guidelines provided for inclusion in the International Reactor Physics Experiment Evaluation Project Handbook. Results provided include updated evaluation of the initial six cold critical core configurations (five annular and one fully-loaded). The calculated $k_{eff}$ eigenvalues agree within ~3σ of the benchmark values and are approximately 2% greater than the benchmark values. Reactor physics measurements that were evaluated include reactivity effects measurements such as excess reactivity during the core loading process and shutdown margins for the fully-loaded core, six isothermal temperature reactivity coefficient measurements for the fully-loaded core, and axial reaction rate measurements in the instrumentation columns of three core configurations. The calculated values agree well with the benchmark experiment measurements. Fully subcritical and warm critical configurations of the fully-loaded core were also assessed. The calculated $k_{eff}$ eigenvalues for these three configurations also agree within ~3σ of the benchmark values. Results are comparable with those obtained in Japanese evaluations. The reactor physics measurement data can be used in the validation and design development of future High Temperature Gas-cooled Reactor systems.

*Key Words*: benchmark, HTTR, graphite reactor, prismatic fuel, TRISO

## 1. INTRODUCTION

The evaluation of Japan's 30 MWt High Temperature Engineering Test Reactor (HTTR) is one of the high priority benchmarking activities for the Next Generation Nuclear Plant (NGNP) Project and the Very High Temperature Reactor (VHTR) Program. The HTTR is currently operational with prismatic-block low-enriched TRISO fuel, graphite moderation, and helium coolant. Reactor physics measurement data were obtained during the initial start-up core tests that can be used in the validation and design development of future High Temperature Gas-cooled Reactors (HTGRs).

Collaboration through the International Atomic Energy Agency (IAEA) provided a mixture of computational analysis results regarding experimental measurements obtained during the initial start-up core tests [1]. Further reevaluations were performed by the Japanese to reduce the discrepancy between the experimental measurements and the computationally-estimated results [2-3]. Recent activities at the Idaho National Laboratory (INL) included the use of Monte Carlo N-Particle version 5 (MCNP5) [4] with ENDF/B-VII.0 nuclear data libraries [5] to develop a comprehensive benchmark evaluation of the initial HTTR reactor physics experiments in conjunction with the International Reactor Physics Experiment

Evaluation Project (IRPhEP) for the verification and validation of VHTR Program methods and inclusion in the IRPhEP Handbook [6]. The benchmark models of the criticality conditions for the fully-loaded [7-8] and annular core loadings [9-10] have been previously assessed and addressed. The concluding benchmark analyses for the HTTR start-up core, which are discussed here in this report, include additional reactivity effects, reactivity coefficient, and reaction-rate distribution measurements.

## 2. BENCHMARK MODEL DEVELOPMENT

The active HTTR core has a height of 290 cm, an effective diameter of 230 cm, and contains a total of 30 fuel columns (Figures 1 and 2). Each column consists of five hexagonal IG-110 graphite fuel blocks with a height of 58 cm and flat-to-flat distance of 36 cm. Control rod guide blocks, replaceable reflector blocks, and irradiation blocks have the same dimensions; all blocks are stacked vertically within the core. Prismatic fuel compacts containing low enriched (~6 wt.% on average across the core) uranium-dioxide TRISO particles are placed within graphite sleeves and inserted into channels within the fuel blocks. Sixteen pairs of boron carbide control rods are utilized to maintain reactivity control. Dummy fuel blocks comprised of IG-11 graphite were initially placed within the core and were replaced with IG-110 graphite fuel blocks during the reactor fueling stages of the start-up tests. A radial reflector of PGX graphite surrounds the reactor core.

Select public references [1-3, 11-14] provide dimensions, compositions, and uncertainties utilized in the development and subsequent assessment of the HTTR benchmark models. Additional guidance was provided by Nozomu Fujimoto, from the Oarai Research Development Center of the Japan Atomic Energy Agency (JAEA), to illuminate understanding of available information and improve final benchmark assessment results.

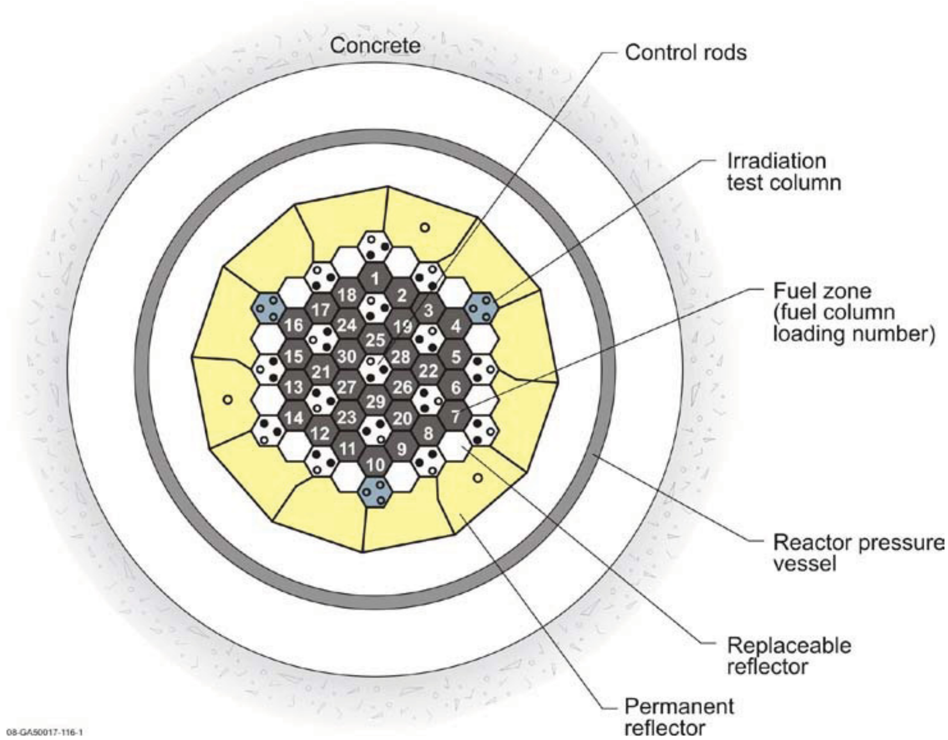


**Figure 1. Horizontal Cross Section of the HTTR.**

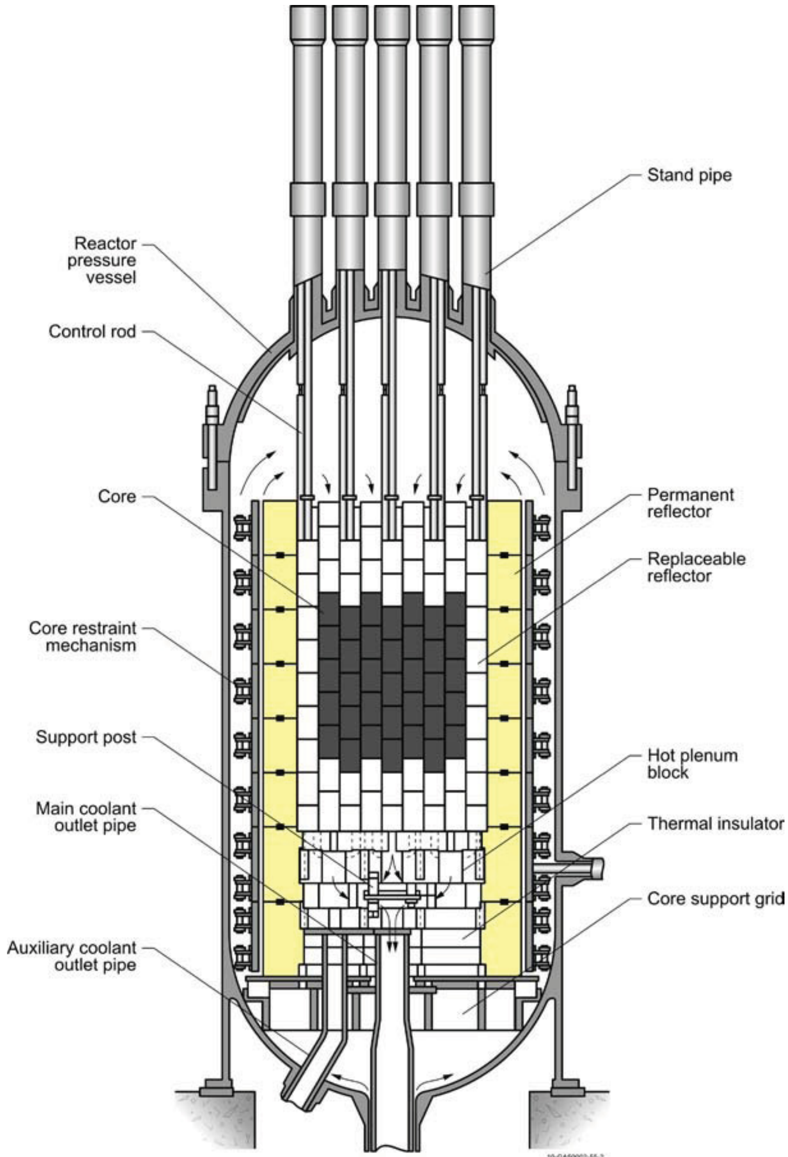


**Figure 2. Vertical Cross Section of the HTTR.**

## 2.1. Improvement of Critical Core Configuration Benchmarks

Initial assessment of the HTTR cold critical configurations (annular and fully-loaded) resulted in computational biases between +2-3% [8, 10]. It was initially believed that this discrepancy was driven by uncertainties in the impurity composition of the graphite components of the reactor because of the sensitivity of the benchmark model to the graphite impurity. Japanese evaluations have also shown discrepancy in calculations of the HTTR due to cross section data for $^{235}$U and graphite [15, 16]. An additional assessment to account for the removal of instrumentation from the instrumentation columns was quantified. The effective bias in removing the instrumentation from the benchmark model had a more significant impact upon the annular configurations of the core than on the fully-loaded core configuration.

The total uncertainty in the benchmark models have been reduced as additional information regarding the manufacturing tolerances of graphite components and uranium fuel enrichment. Unfortunately, information regarding the actual uncertainty, and not the tolerance limits, of impurities in the graphite blocks of the HTTR remain unavailable. The uncertainty in the impurity content of the IG-11, IG-110, and PGX graphites still dominate the total uncertainty in the benchmark $k_{eff}$ eigenvalues. The improvements to the critical core configurations have been updated in the existing IRPhEP benchmark reports [7, 9].

## 2.2. Reactor Physics Experimental Measurements

Additional reactor physics measurements were obtained during the start-up and zero-power core physics tests. Reactivity effects measurements include core excess reactivity throughout the core loading process as well as the partial and total shutdown margin measurements for the fully-loaded core. The isothermal temperature coefficient was measured for temperatures ranging between approximately 70 and 500 ºC. Fission chambers placed in the irradiation test columns were used to measure the axial reaction rates in the annular, 24-fuel-column core (two control rod patterns) and the fully-loaded core [1, 11-12, 14]. It should be noted that the isothermal temperature coefficients found in the IAEA benchmark study [1] were provided for evaluation purposes only and do not represent actual core measurements.

## 2.3. Additional Eigenvalue Measurements

An effective multiplication factor of 0.685 ± 0.010 was reported for the fully subcritical condition of the fully-loaded core configuration, with all control rods fully inserted. Control rods are considered fully inserted when the bottom of the rod is level with the bottom plane of the fueled region of the core; they considered fully withdrawn at a height of approximately 405 cm above this plane. The conditions for criticality were also assessed and reported for two warm critical conditions of the fully-loaded core configuration at isothermal temperatures of 122.0 and 144.9ºC. The center, R1, and R2 control rods were all withdrawn to a height of 187.3 and 190.0 cm, respectively, and the R3 control rods were completely withdrawn [14]. The warm critical configuration reported at 480 K in the IAEA benchmark study [1] was provided for evaluation purposes only and does not represent an actual core measurement.

# 3. RESULTS AND DISCUSSION

## 3.1. Revised Criticality Benchmark Eigenvalues

The updated criticality benchmark eigenvalues, $k_B$, for the five annular and one fully-loaded core configurations of the HTTR are provided in Table I. The uncertainties in the benchmark model eigenvalues are provided, as are the calculated eigenvalues, $k_C$. The benchmark eigenvalues represent the experimental eigenvalues ($k_{eff}$ = 1.0000) that have been adjusted for the removal of instrumentation used during the actual experiment. Computed eigenvalues are within the one-sigma uncertainty of the benchmark values. All six critical configurations were performed at room temperature, approximately 300 K.

The difference between the calculated and benchmark values is ~2%Δk and slightly less than previously calculated values. These results are slightly greater than the most recent results reported by the Japanese using the MVP Monte Carlo code and JENDL-3.2 nuclear data library [11]. Uncertainties in the experimentally measured eigenvalues were not provided in the Japanese analysis, however. Monte Carlo analyses performed with JENDL-3.3 data have less computational bias [7, 9] due to some differences in cross section data for $^{235}$U and graphite; the use of different cross section libraries can introduce a discrepancy of up to ~0.5%$\Delta k_{eff}$ [15]. Other studies have shown that the resonance scattering treatment in MCNP may need modified to improve eigenvalue calculations for large graphite systems [17].

**Table I. Calculated and Benchmark Eigenvalues for Critical Configurations of the HTTR.**

| Loaded Fuel Columns | Control Rod Configuration[(a)] | Benchmark | | | Calculated | | | $\frac{k_C - k_B}{k_B}(\%)$ |
|---|---|---|---|---|---|---|---|---|
| | | $k_B$ | ± | 1σ | $k_C$ | ± | 1σ | |
| 19 | Central | 1.0048 | ± | 0.0103 | 1.0276 | ± | 0.0001 | 2.27 |
| 21 | Flat Standard | 1.0040 | ± | 0.0100 | 1.0297 | ± | 0.0001 | 2.55 |
| 24 | Flat Standard | 1.0035 | ± | 0.0084 | 1.0249 | ± | 0.0001 | 2.13 |
| 24 | Radial Reflectors | 1.0032 | ± | 0.0080 | 1.0287 | ± | 0.0001 | 2.54 |
| 27 | Flat Standard | 1.0029 | ± | 0.0075 | 1.0218 | ± | 0.0001 | 1.88 |
| 30 | Flat Standard | 1.0025 | ± | 0.0071 | 1.0229 | ± | 0.0001 | 2.03 |

[(a)] Criticality is obtained using one of three methods (see Figure 3 for control rod locations):

- the Central pattern where the C control rods are inserted and all other control rods are all fully withdrawn,
- the Flat Standard pattern where the C, R1, and R2 control rods are inserted to the same depth in the core and the R3 control rods are fully withdrawn, and
- the Radial Reflectors pattern where the C and R1 control rods are completely withdrawn and the R2 and R3 rods in the reflector region are inserted to the same depth.

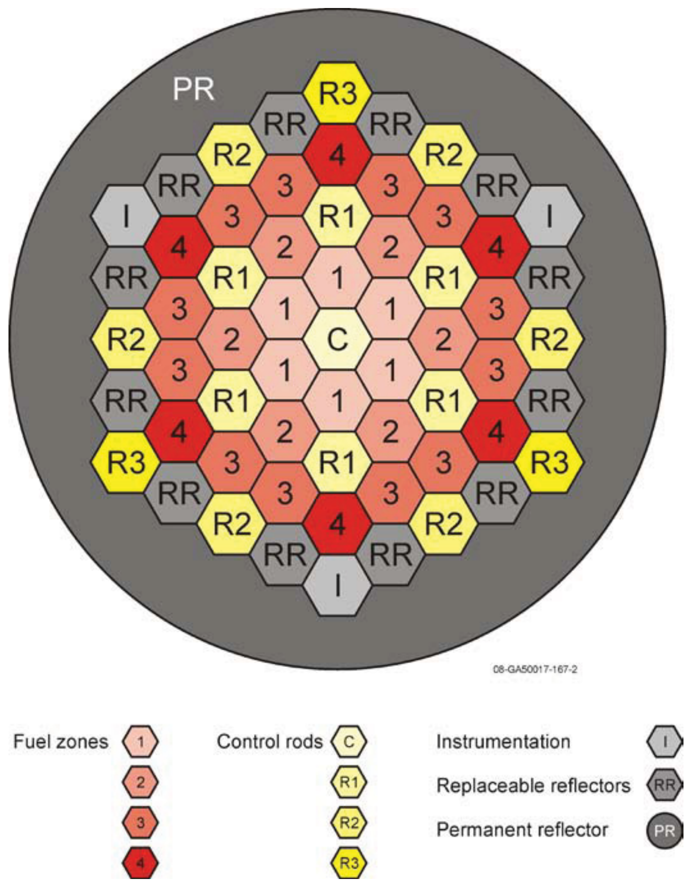


**Figure 3. Core Positions in the HTTR.**

## 3.2. Evaluation of the Excess Reactivity Measurements

The excess reactivity of the core was obtained by measuring and adding all fuel loading increments from initial criticality (19 fuel columns) to the fully-loaded core (30 fuel columns). The excess reactivity of the initial critical was determined from the cumulative worth of the subcritical, 18-fuel-column and the critical, 19-fuel-column core configurations. A comparison of the benchmark experiment excess reactivity values, $\rho_B$, and the calculated values, $\rho_C$, for the individual and cumulative excess reactivity measurements are provided in Tables II and III, respectively. The calculated values generally appear to compare well against the benchmark experiment values, within approximately 8%, except for the cumulative excess reactivity of the 19- and 30-fuel-column cores. Results compare well with the aforementioned Monte Carlo analysis [11] and compare better than a diffusion theory analysis of the HTTR core [12].

**Table II. Individual Excess Reactivity Measurements for the HTTR.**

| Loaded Fuel Columns | Benchmark $\Delta\rho_B$ (%Δk/k) | Calculated $\Delta\rho_C$ (%Δk/k) | $\rho_C/\rho_B$ |
|---|---|---|---|
| 19 | -- | -- | -- |
| 21 | -- | 2.30 ± 0.01 | -- |
| 24 | 3.7 ± 1.0 | 4.01 ± 0.02 | 1.08 |
| 27 | 3.0 ± 0.9 | 3.23 ± 0.02 | 1.08 |
| 30 | 1.3 ± 0.3 | 1.30 ± 0.01 | 1.00 |

**Table III. Cumulative Excess Reactivity Measurements for the HTTR.**

| Loaded Fuel Columns | Benchmark $\rho_B$ (%Δk/k) | Calculated $\rho_C$ (%Δk/k) | $\rho_C/\rho_B$ |
|---|---|---|---|
| 19[(a)] | 2.4 ± 0.24 | 1.98 ± 0.02 | 0.83 |
| 21 | 4.0 ± 1.1 | 4.28 ± 0.02 | 1.07 |
| 24 | 7.7 ± 2.1 | 8.29 ± 0.03 | 1.08 |
| 27 | 10.7 ± 3.0 | 11.52 ± 0.03 | 1.08 |
| 30 | 12.0 ± 3.3 | 11.38[(b)] ± 0.01 | 0.95 |

[(a)] This value represents the cumulative worth of fuel addition from the subcritical 18-fuel-column and the critical 19-fuel-column core configurations.
[(b)] This value represents the excess reactivity calculated by completely withdrawing all control rods from the fully-loaded 30-fuel-column core configuration.

## 3.3. Evaluation of the Shutdown Margin Measurements

There are three shutdown margin benchmark measurements for the fully-loaded core:

1. Full insertion of the radial reflector control rods, R2 and R3, from the critical configuration,
2. Full insertion of the fuel region control rods, C and R1, from the previous configuration, and
3. Full insertion of all control rods from the critical configuration.

All three shutdown margin measurements were evaluated and a comparison of the benchmark experiment shutdown margins, $\rho_B$, with the calculated values, $\rho_C$, is provided in Table IV. Results are comparable to those previously obtained using a diffusion theory analysis [12].

**Table IV. Shutdown Margin Measurements for the Fully-Loaded HTTR Core.**

| | Configuration | Benchmark $\rho_B$ (%Δk/k) | Calculated $\rho_C$ (%Δk/k) | $\rho_C/\rho_B$ |
|---|---|---|---|---|
| 1 | Insertion of Control Rods in Reflector Region | -12.1 ± 0.6 | -9.27 ± 0.02 | 0.77 |
| 2 | Insertion of Control Rods in Fuel Region | -34.2 ± 1.7 | -37.31 ± 0.03 | 1.09 |
| 3 | Insertion of All Control Rods | -46.3 ± 1.2 | -46.59 ± 0.03 | 1.01 |

## 3.4. Evaluation of the Isothermal Temperature Coefficient Measurements

The isothermal temperature reactivity coefficient measurements for the fully-loaded core configuration of the HTTR were reported for six temperatures, with multiple measurements performed at three of the temperatures. A comparison of the benchmark experiment isothermal temperature coefficient values, $\rho_B$, and the calculated values, $\rho_C$, is provided in Table V and Figure 4. The first three calculated coefficients are within 1σ of the benchmark value. The fourth and fifth coefficients are within 4σ and 3σ, respectively. The last coefficient is within 13σ, and may require further evaluation. Control rod positions were estimated for the coefficients at temperatures above 420 K using worth data from Reference 12. The uncertainty in the third coefficient is very large, possibly due to experimental measurement uncertainty, and it does not provide significant worth as a benchmark value.

**Table V. Isothermal Temperature Coefficient Measurements for the Fully-Loaded HTTR Core.**

| Temperature (K) | Benchmark $\rho_B$ (%Δk/k/K) | Calculated $\rho_C$ (%Δk/k/K) | $\rho_C/\rho_B$ |
|---|---|---|---|
| 346 | -0.0123 ± 0.0018 | -0.0116 ± 0.0001 | 0.94 |
| 407 | -0.0132 ± 0.0020 | -0.0129 ± 0.0001 | 0.98 |
| 421 | -0.0217 ± 0.0127 | -0.0128 ± 0.0001 | 0.59 |
| 533 | -0.0165 ± 0.0011 | -0.0129 ± 0.0001 | 0.78 |
| 642 | -0.0103 ± 0.0008 | -0.0125 ± 0.0001 | 1.21 |
| 736 | -0.0086 ± 0.0003 | -0.0120 ± 0.0001 | 1.40 |

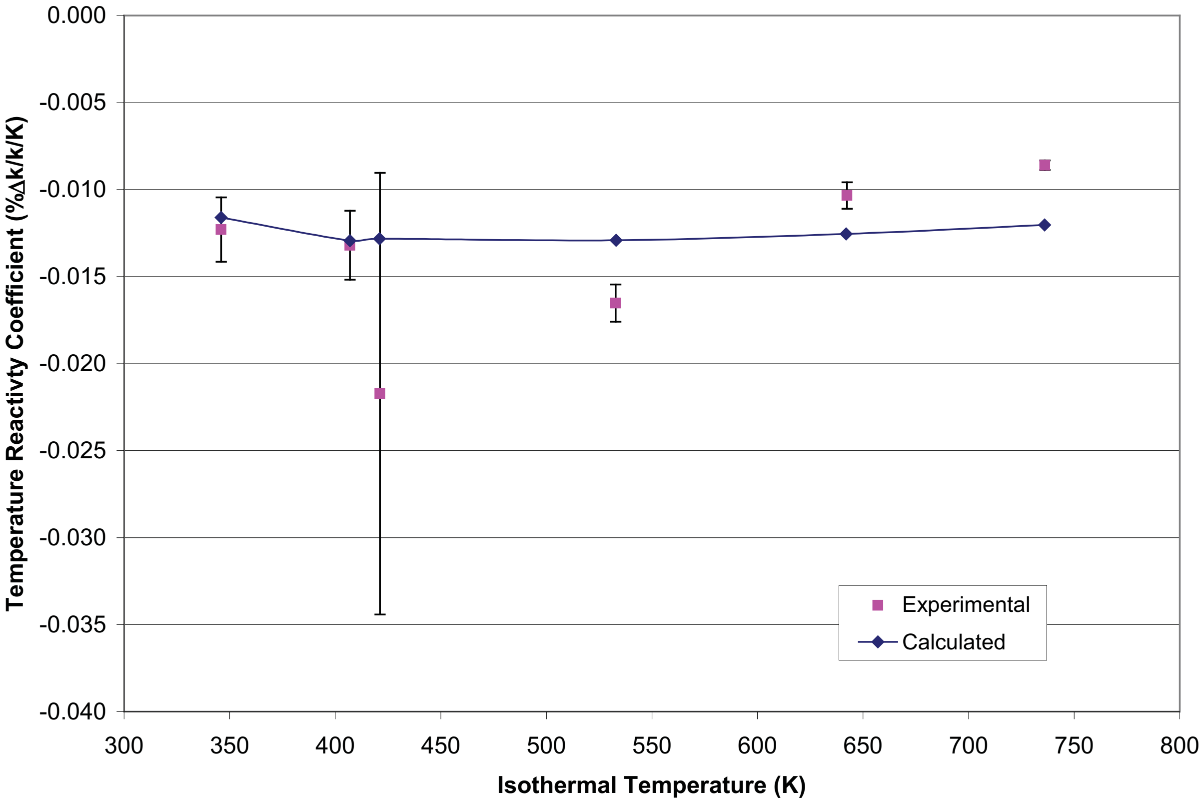


**Figure 4. Isothermal Temperature Coefficients for Fully-Loaded HTTR Core.**

### 3.5. Evaluation of the Axial Reaction Rate Measurements

The reaction rate of $^{235}U$ was directly measured in the HTTR core axially along the instrumentation columns and then normalized and used to represent the neutron flux. Measurements were performed for three configurations: both configurations of the 24-fuel-column core configuration as well as the fully-loaded core configuration. A comparison of the benchmark experiment reaction rate values, $R_B$, to the calculated values, $R_C$, are provided in Table VI. The comparison is visually shown for the fully-loaded core configuration in Figure 5. A with previous Monte Carlo [11] and diffusion theory analyses [12], there is a good fit between calculated and experimental reaction rates.

**Table VI. Axial Reaction Rate Measurements in the Instrumentation Columns of the HTTR.**

| Core and Control Rod Configuration[(a)] | Height (cm)[(b)] | Benchmark $R_B$ | ± | 1σ | Calculated $R_C$ | ± | 1σ | $R_C/R_B$ |
|---|---|---|---|---|---|---|---|---|
| 1 24-Fuel-Column Flat Standard | 18.89 | 0.6946 | ± | 0.0199 | 0.6914 | ± | 0.0014 | 0.995 |
| | 27.86 | 0.7304 | ± | 0.0198 | 0.7326 | ± | 0.0014 | 1.003 |
| | 86.07 | 0.9555 | ± | 0.0173 | 0.9650 | ± | 0.0016 | 1.010 |
| | 130.96 | 1.0000 | ± | 0.0166 | 1.0000 | ± | 0.0016 | 1.000 |
| | 137.15 | 0.9854 | ± | 0.0169 | 0.9892 | ± | 0.0016 | 1.004 |
| | 143.96 | 0.9750 | ± | 0.0170 | 0.9761 | ± | 0.0016 | 1.001 |
| | 202.48 | 0.6735 | ± | 0.0200 | 0.6894 | ± | 0.0014 | 1.024 |
| | 260.99 | 0.2818 | ± | 0.0165 | 0.3043 | ± | 0.0009 | 1.080 |
| | 318.58 | 0.1041 | ± | 0.0095 | 0.1111 | ± | 0.0005 | 1.068 |
| 2 24-Fuel-Column Radial Reflectors | 18.79 | 0.7030 | ± | 0.0199 | 0.6932 | ± | 0.0015 | 0.986 |
| | 28.40 | 0.7383 | ± | 0.0197 | 0.7380 | ± | 0.0016 | 1.000 |
| | 86.36 | 0.9523 | ± | 0.0174 | 0.9625 | ± | 0.0018 | 1.011 |
| | 115.79 | 1.0000 | ± | 0.0166 | 1.0000 | ± | 0.0018 | 1.000 |
| | 137.45 | 0.9749 | ± | 0.0170 | 0.9704 | ± | 0.0018 | 0.995 |
| | 144.57 | 0.9562 | ± | 0.0173 | 0.9569 | ± | 0.0018 | 1.001 |
| | 202.72 | 0.7915 | ± | 0.0193 | 0.7905 | ± | 0.0016 | 0.999 |
| | 260.85 | 0.5582 | ± | 0.0201 | 0.5625 | ± | 0.0014 | 1.008 |
| | 318.37 | 0.3312 | ± | 0.0176 | 0.3417 | ± | 0.0011 | 1.032 |
| 3 30-Fuel-Column Flat Standard | 19.68 | 0.8381 | ± | 0.0127 | 0.8307 | ± | 0.0013 | 0.991 |
| | 28.47 | 0.8759 | ± | 0.0126 | 0.8650 | ± | 0.0014 | 0.988 |
| | 71.81 | 0.9991 | ± | 0.0128 | 0.9918 | ± | 0.0015 | 0.993 |
| | 82.53 | 1.0000 | ± | 0.0116 | 1.0000 | ± | 0.0015 | 1.000 |
| | 56.52 | 0.9784 | ± | 0.0242 | 0.9989 | ± | 0.0015 | 1.021 |
| | 93.61 | 0.9703 | ± | 0.0306 | 0.9920 | ± | 0.0015 | 1.022 |
| | 144.22 | 0.7673 | ± | 0.0277 | 0.7981 | ± | 0.0013 | 1.040 |
| | 202.28 | 0.3695 | ± | 0.0158 | 0.4070 | ± | 0.0009 | 1.101 |
| | 261.19 | 0.1302 | ± | 0.0094 | 0.1505 | ± | 0.0006 | 1.156 |
| | 319.13 | 0.0440 | ± | 0.0057 | 0.0552 | ± | 0.0004 | 1.255 |

(a) See Table I for an explanation of the control rod configurations.
(b) The height is relative to the bottom of the fifth layer of fuel.

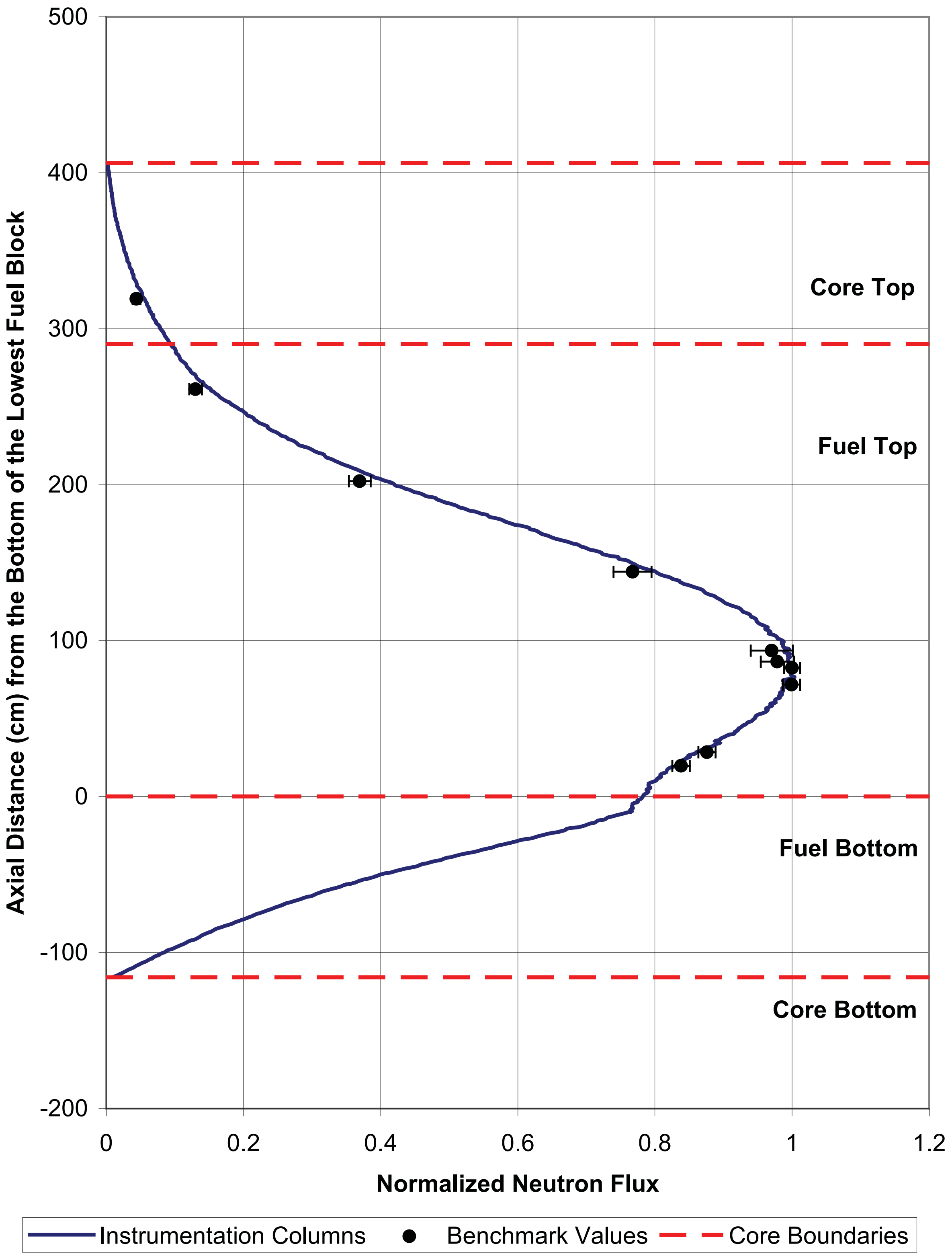


**Figure 5. Axial Reaction Rate Measurements for Fully-Loaded Core Configuration.**

### 3.6. Additional Eigenvalue Measurements

The benchmark eigenvalues, $k_B$, for the fully subcritical and warm critical configurations of the fully-loaded HTTR core are provided in Table VII. The uncertainty in the benchmark model eigenvalues are provided, as are the calculated eigenvalues, $k_C$. The benchmark eigenvalues represent the experimental eigenvalues ($k_{eff}$ = 1.0000) that have been adjusted for the removal of instrumentation used during the actual experiment. Computed eigenvalues are within the 3σ of the benchmark values, with computational biases also on the order of ~2%, as seen in the cold critical benchmarks.

**Table VII. Calculated and Benchmark Eigenvalues for Additional Configurations of the HTTR.**

| Loaded Fuel Columns (Temperature) | Control Rod Configuration[a] | Benchmark | | | Calculated | | | $\frac{k_C - k_B}{k_B}(\%)$ |
|---|---|---|---|---|---|---|---|---|
| | | $k_B$ | ± | 1σ | $k_C$ | ± | 1σ | |
| 30 (300 K) | Fully Subcritical | 0.6876 | ± | 0.0011 | 0.6999 | ± | 0.0001 | 1.78 |
| 30 (400 K) | Flat Standard | 1.0025 | ± | 0.0068 | 1.0195 | ± | 0.0001 | 1.69 |
| 30 (420 K) | Flat Standard | 1.0024 | ± | 0.0067 | 1.0197 | ± | 0.0001 | 1.72 |

[a] Control rod positions are explained as follows (see Figure 3 for control rod locations):

- the Fully Subcritical pattern where all control rods are fully inserted, and
- the Flat Standard pattern where the C, R1, and R2 control rods are inserted to the same depth in the core and the R3 control rods are fully withdrawn.

## 4. CONCLUSIONS

Benchmark assessment of the start-up core reactor physics measurements performed with Japan's HTTR, in support of NGNP Project and VHTR Program activities at the INL, have been completed using MCNP5 with ENDF/B-VII.0. The results have been documented in IRPhEP benchmark reports. Evaluated measurements include six cold critical core configurations (five annular and one fully-loaded), excess reactivity measurements during core loading, shutdown margins for the fully-loaded core, isothermal temperature coefficient measurements for the fully-loaded core, axial reaction rate measurements in the instrumentation columns of three core configurations, and subcritcal and two warm critical configurations of the fully-loaded core.

Uncertainties and computational biases for the six cold critical configurations published in previous reports have been slightly reduced, providing higher fidelity benchmark models. Analyses were satisfactory with $k_{eff}$ eigenvalue calculations within 3σ of the benchmark values; the largest sources of uncertainty remain from graphite impurities and differences in graphite cross sections. Reactor physics measurements were also determined to be of good benchmark value. Benchmark models of the subcritical and two warm critical fully-loaded core configurations were also evaluated.

Remaining work includes the final submission of the isothermal temperature coefficient and warm critical benchmark analyses to the IRPhEP for inclusion in the Handbook. The reactor physics measurement data from the HTTR start-up and core physics tests can be used in the validation and design development of future HTGRs.

## ACKNOWLEDGMENTS

Funding for the HTTR benchmark was provided by the INL VHTR Program. The author would like to acknowledge the time and expertise provided by Nozomu Fujimoto from the Japan Atomic Energy Agency; Luka Snoj from the Jožef Stefan Institute; Atsushi Zukeran, acting as a senior reactor physics consultant; and Blair Briggs, Barbara Dolphin, Dave Nigg, Jim Sterbentz, and Chris White from the INL, for the review and preparation of the HTTR benchmark reports. This paper was prepared at Idaho National Laboratory for the U.S. Department of Energy under Contract Number (DE-AC07-05ID14517).

## REFERENCES

1. IAEA, "Evaluation of High Temperature Gas Cooled Reactor Performance: Benchmark Analysis Related to Initial Testing of the HTTR and HTR-10," IAEA-TECDOC-1382 (2003).
2. K. Yamashita, et al., "Startup Core Physics Tests of High Temperature Engineering Test Reactor (HTTR), (I)," *J. At. Energy Soc. Jpn.*, **42**, pp. 30-42 (2000) [in Japanese].
3. N. Fujimoto, et al., "Start-Up Core Physics Tests of High Temperature Engineering test Reactor (HTTR) (II)," *J. At. Energy Soc. Jpn.*, **42**, pp. 458-464 (2000) [in Japanese].
4. F. B. Brown, et al., "MCNP Version 5," LA-UR-02-3935, Los Alamos National Laboratory (2002).
5. M. B. Chadwick, et al., "ENDF/B-VII.0: Next Generation Evaluated Nuclear Data Library for Nuclear Science and Technology," *Nucl. Data Sheets*, **107**, 2931 (2006).
6. *International Handbook of Evaluated Reactor Physics Benchmark Experiments*, NEA/NSC/DOC(2006)1, OECD-NEA, March (2009).
7. J. D. Bess and N. Fujimoto, "Evaluation of the Start-Up Core Physics Tests at Japan's High Temperature Engineering Test Reactor (Fully-Loaded Core)," HTTR-GCR-RESR-001, revision 1, *International Handbook of Evaluated Reactor Physics Benchmark Experiments*, NEA/NSC/DOC(2006)1, OECD-NEA, March (2010).
8. J. D. Bess, "Preliminary Benchmark Evaluation of Japan's High Temperature Engineering Test Reactor," *Proc. International Conference on Mathematics, Computational Methods & Reactor Physics (M&C 2009)*, Saratoga Springs, NY, May 3-7 (2009).
9. J. D. Bess and N. Fujimoto, "Evaluation of the Start-Up Core Physics Tests at Japan's High Temperature Engineering Test Reactor (Annular Core Loadings)," HTTR-GCR-RESR-002, *International Handbook of Evaluated Reactor Physics Benchmark Experiments*, NEA/NSC/DOC(2006)1, OECD-NEA, March (2010).
10. J. D. Bess, "Criticality Benchmark Analysis of the HTTR Annular Startup Core Configurations," *Trans. Am. Nucl. Soc.*, **101**, pp. 806-807 (2009).
11. N. Fujimoto, et al., "Annular Core Experiments in HTTR's Start-Up Core Physics Tests," *Nucl. Sci. Eng.*, **150**, pp. 310-321 (2005).
12. "Topical Issue on Japan's HTTR," *Nucl. Eng. Des.*, **233**, pp. 1-407 (2004).
13. S. Saito, et al., "Design of High Temperature Test Reactor (HTTR)," JAERI 1332, Japan Atomic Energy Research Institute, September (1994).
14. N. Fujimoto, et al., "Control Rod Position and Temperature Coefficients in HTTR Power-Rise Tests: Interim Report," JAERI Tech 2000-091, Japan Atomic Energy Agency (2001) [in Japanese].
15. M. Goto, N. Nojiri, and S. Shimakawa, "Neutronics Calculations of HTTR with Several Nuclear Data Libraries," *J. Nucl. Sci. Technol.*, **43**, pp. 1237-1244 (2006).
16. S. Shimakawa and K. Kunitomi, "Validation of Reactor Physics Codes Used for HTTR and Design-Phase HTGRs at JAEA," Verification and Validation for Nuclear Systems Analysis Workshop, Idaho Falls, Idaho, July 21-25 (2008).
17. B. Becker, et al., "Improvements of the Resonance Scattering Treatment in MCNP in View of HTR Calculations," *Ann. Nucl. Energy*, **36**, pp. 281-285 (2009).